First Principle Study of Electronic Structure, Chemical Bonding and Optical Properties of 5-azido-1H-tetrazole

Saleem Ayaz Khan[1], A. H. Reshak[1,2,]*

[1] Institute of complex systems, FFPW, CENAKVA, University of South Bohemia in CB, Nove Hrady 37333, Czech Republic
[2] Center of Excellence Geopolymer and Green Technology, School of Material Engineering, University Malaysia Perlis, 01007 Kangar, Perlis, Malaysia
[*]E-mail: maalidph@yahoo.co.uk

First principle calculations were performed to investigate the electronic band structure, density of states, charge density and optical properties of 5-azido-1H-tetrazole. The calculated band structure shows that the compound is a semiconductor having indirect $(\Gamma \rightarrow A_0)$ band gap. The total valance charge density in $(\overline{4}0\overline{9})$ plane shows the covalent nature of the bonds in 5-azido-1H-tetrazole molecule. The compound 5-azido-1H-tetrazole contains four homodimers. In each homodimer the molecules held together by hydrogen bond of about 1.74 Å. The calculated bond length, angles and torsion angles of 5-azido-1H-tetrazole show close agreement with experimental results. The average value of real and imaginary part of dielectric function was calculated. The three principal tensor components of $\varepsilon_2(\omega)$, $\varepsilon_1(\omega)$, $n(\omega)$, $I(\omega)$ and $R(\omega)$ were investigated. The calculated band gap's values and optical properties show that the investigated compound is suitable for optoelectronic devices in far-ultraviolet (UV-C) region.

1. INTRODUCTION

In recent years the energetic heterocyclic compounds like pyrimidines, triazoles, triazines, tetrazoles, tetrazines and heptazines [1] gain considerable attention due to their vast application in civil and military areas [2-10]. Some of azole and tetrazole derivatives used as corrosion inhibitive in copper, aluminum [11,12]. The study of tetrazole compounds is linked to the application of nitrogen nuclear quadrupole resonance (^{14}N NQR) to detect explosives and the study of polymorphism in some pharmaceuticals [13]. Previous literature on tetrazole derivatives shows that 5-substituted tetrazoles

show more stability than 1–and 2–substituted isomers [14]. Among them 5-azido-1*H*-tetrazole is new energetic materials [15-18]. It belongs to the group which contains the highest nitrogen content [19, 20]. Due to high nitrogen percentage the 5-azido-1*H*-tetrazole has further vast applications including effective precursors for carbon nanospheres and carbon nitride nanomaterials, [21-23] solid fuels in micropropulsion systems [24], gas generators [25], and smoke-free pyrotechnic fuels [26]. A lot of work has been done on structure properties and decomposition mechanism of this group of compounds [2, 5, 14, 7, 27-34]. The 5-azido-1*H*-tetrazole exhibit high density, good thermal stability and high positive heat formation, low sensitivities towards impact and friction, both 5-azido-1*H*-tetrazole and its decomposition product are compatible for environment [19, 34]. Though 5-azido-1*H*-tetrazole was found to be very sensitive for applications, it is still an attractive compound for researchers because the detailed decomposition mechanism by which the solids release energy under mechanical shock is still not well understood [34].

For the first time in 1939 the neutral 5-azido-1*H*-tetrazole was expressed in patents [35, 36] and was also investigated few years ago [37, 38]. The complete characterization of this compound was not described well due to its erratic explosive nature. Additionally, due to the uncertain position of hydrogen atom in the solution of the crystal structure reported previously was poor.

Stierstorfer et al. [19] determined the crystal structure of 5-azido-1*H*-tetrazole by low temperature X-ray diffraction. They conformed the position of the hydrogen atom contacting the nitrogen atom N_1 by a strong hydrogen bond. The gas phase structures of 5-azido-1*H*-tetrazole and 5-azido-2*H*-tetrazole were compared by DFT calculations using the program package Gaussian03 [39]. Stierstorfer et al. [19] also calculated the heat of formation, thermal behavior, sensitivity, density and several detonation parameters of 5-azido-1*H*-tetrazole using EXPLO5 software [40], differential scanning calorimetry (DSC) [41] and BAM drophammer [42, 43], ESD and friction tester.

To understand the explosive properties of crystalline 1H-tetrazole and its substituted derivatives 5-amino-1H-tetrazole\ 5-methyl-1H-tetrazole\5-azido-1H-tetrazole Zhu et al.[34] performed a DFT study of electronic structure, absorption spectra, and thermo-dynamic properties using CASTEP code [44]. They also made to correlate the impact sensitivity of the four crystals with their band gap. Their result shows that the first-principles band gap criterion can be use to predict impact sensitivity for the substituted 1H-tetrazoles. Zhu et al. used Vanderbilt-type ultra-soft pseudo potential method [45] for their calculation which is not much accurate.

In present work we make use of the full potential linear augmented plane wave (FPLAPW) method which has proven to be one of the most accurate methods for the computation of the electronic structure of solids within DFT [46, 47]. Thus we have calculated the electronic band structure, density of state (DOS), bonding nature and optical and properties of 5-azido-1H-tetrazole which give best result as compared to the pseudopotential method.

2. CRYSTAL STRUCTURE AND COMPUTATIONAL DETAIL

The chemical formula of 5-azido-1H-tetrazole is CHN_7. The established crystal structure is monoclinic having space group P21/c, with eight formulas per unit cell . The lattice constant

a=11.560Å, b=7.5553Å, c=17.164Å and β=98.578°, V=1482.3 Å^3, Z=8, μ=0.145mm^{-1}. The crystallographic data for 5-azido-1H tetrazole have been taken from Cambridge Crystallographic data Center [48]. The deposition number for supplementary crystallographic data was (CCDC) 673182. The molecular structure and unit cell of 5-azido-1H-tetrazole are shown in Fig.1.
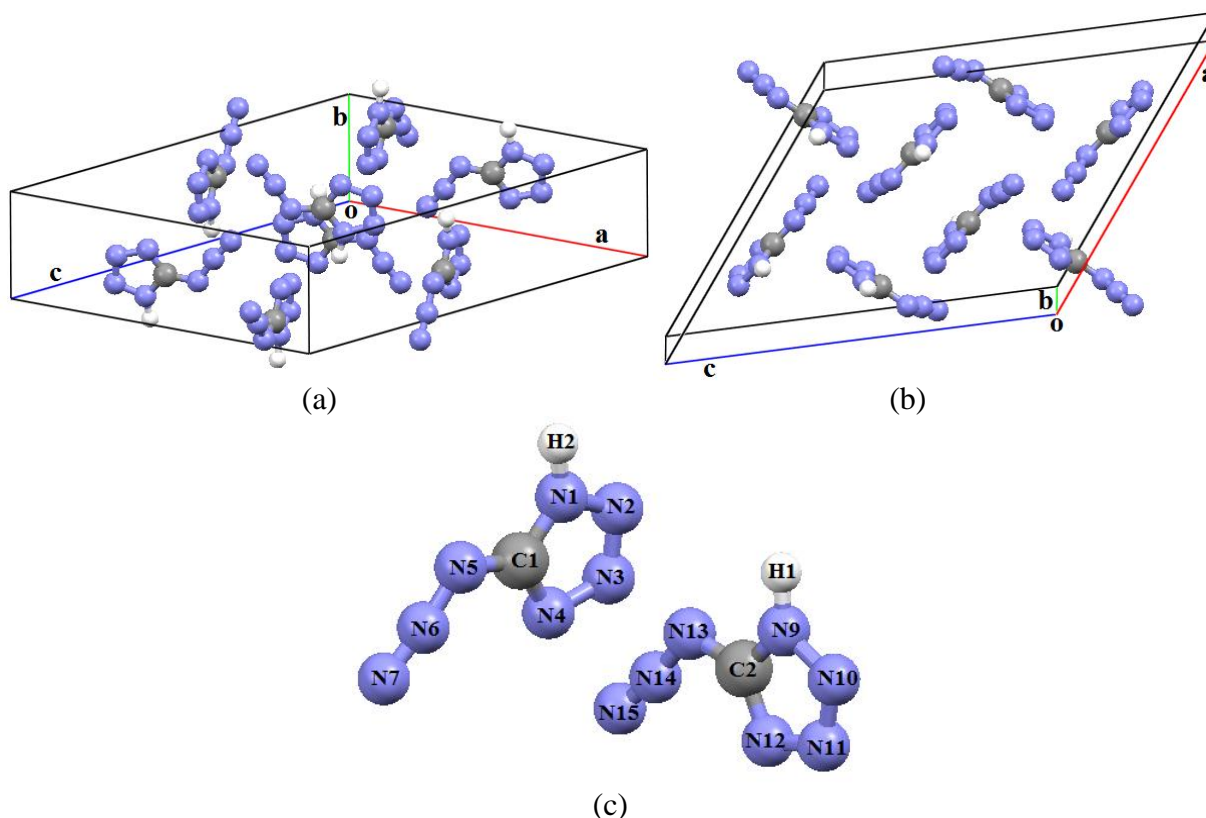
Figure 1. Structure of 5-Azido-1H-tetrazole (a-b) Unit cell (c) Two molecules

The calculations were carried out using the full potential linear augmented plane wave (FPLAPW) method within the frame work of WIEN2K code [49]. The exchange correlation energy was treated by the local density approximation (LDA) using the Ceperley-Alder (CA) approach [50], Generalized gradient approximation (GGA-PBE) [51], and Engle Vasko generalized gradient approximation (EVGGA) [52] for self-consistent calculations. Additionally the most recent modified Becke and Johnson (mBJ) potential was used [53]. For convergence of energy eigenvalues the wave function in the interstitial regions were expended in plane waves with cutoff $R_{MT}K_{max} = 7.0$. Where R_{MT} represent the muffin-tin (MT) sphere radius and K_{max} represent the magnitude of largest K vector in plane wave expansion. The selected R_{MT} are 1.07 atomic units (a.u.) for N, 1.26 a.u. for C and 0.70 a.u. for H atom. The wave function inside the sphere was expended up to $l_{max} = 10$ where as the Fourier expansion of the charge density was up to $G_{max} = 26$ $(a.u.)^{-1}$. The crystal structure is optimized by minimization of forces acting on the atoms. The convergence of the self-consistent calculations were done by the difference in total energy of the crystal did not exceed $10^{-5} Ryd$ for

successive steps. The self consistencies were obtained by 84 **k** points in irreducible Brillion zones (IBZ), initiated from 400 **k** points in the Brillion zones (BZ).

3. RESULT AND DISCUSSION

3.1 Band structure and density of state

The physical properties of many compounds are directly or indirectly correlated to the electronic band structure of the material, while the basis of the band structure can be related to the density of state [54]. In Fig.2 the band structures of 5-zido-1H-tetrazole were calculated using LDA, GGA-PBE, EVGGA and mBJ respectively. The calculated energy gap (E_g) of 5-zido-1H-tetrazole is 3.60 eV (LDA), 3.65 eV (GGA), 3.69 eV (EVGGA), and 4.43 eV (mBJ).
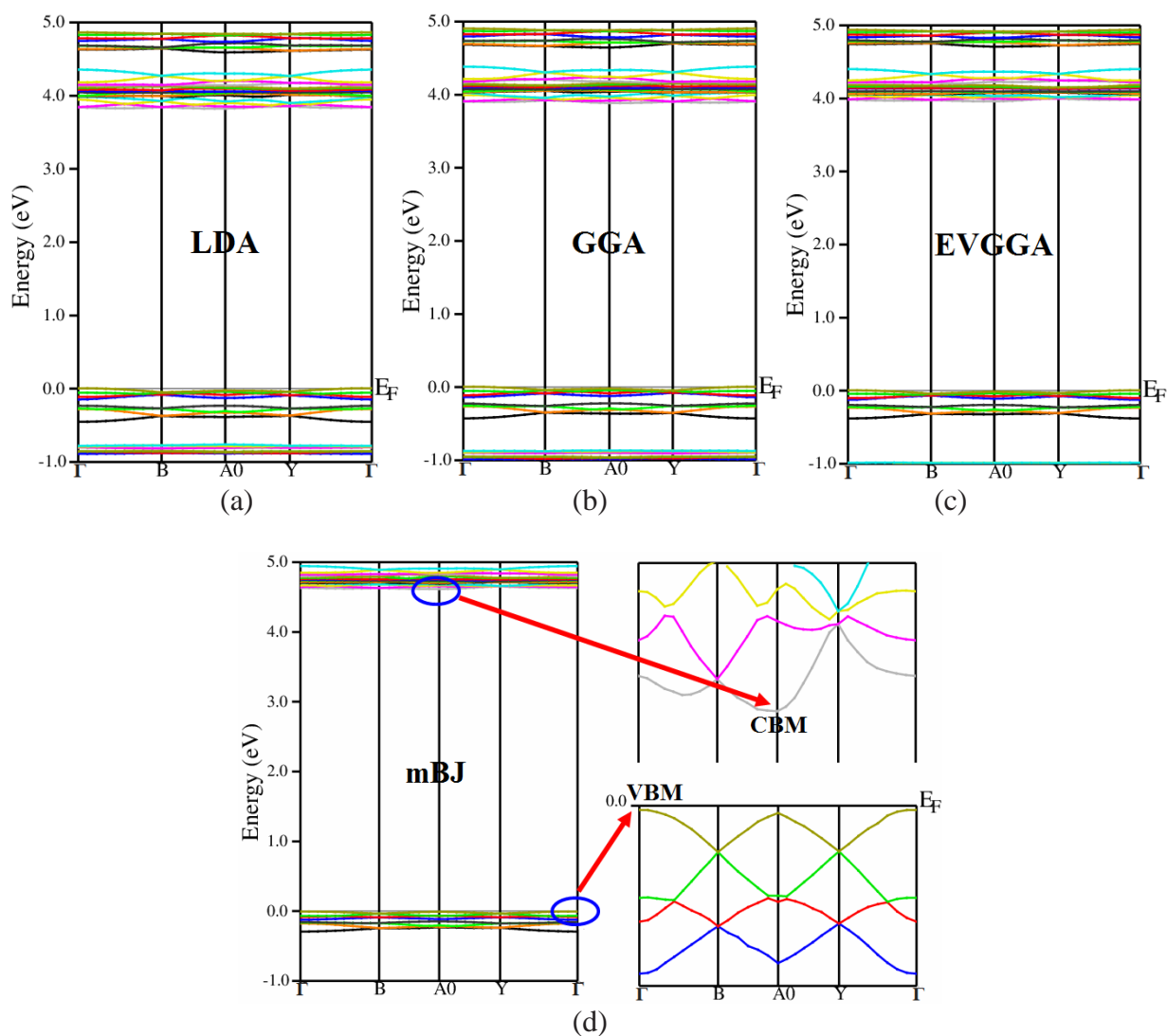
Figure 2. Calculated band structure (a) LDA (b) GGA-PBE (c) EVGGA (d) mBJ

(a)

(b)

(c)
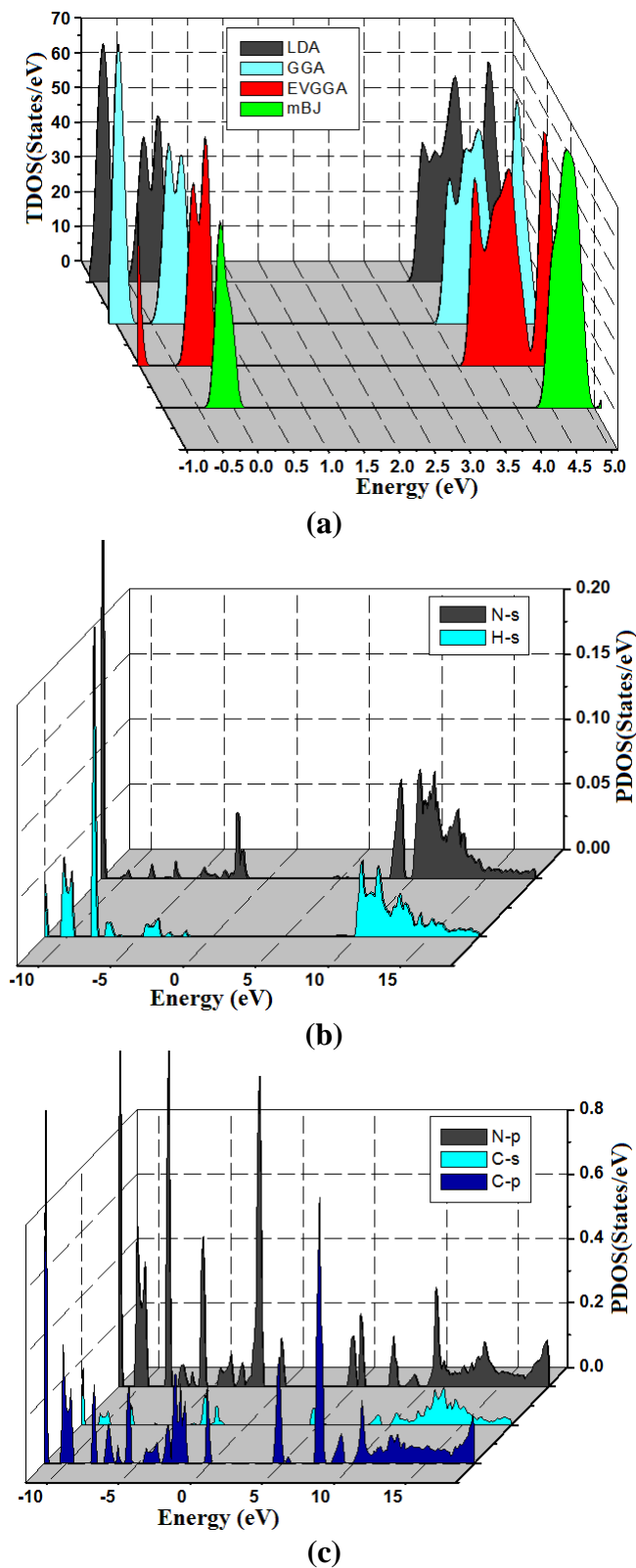
Figure 3. Calculated total and partial densities of states (States/eV unit cell)

Fig.2 and Fig.3a clarifies that mBJ scheme gives better band splitting. The mBJ scheme was selected for further explanation of density of state. To the best of our knowledge there is no

experimental value of the energy gap is available in the literatures. Thus we have compared our calculated energy gap with the previously calculated one (3.82 eV) using CASTEP –LDA [35]. Based on our previous results [55-58] using the FPLAPW method which show good agreement with the experimental data we can consider the present results are more accurate, hoping that our present work will stimulate some more works on this material. Future experimental works will testify our calculated results. In order to study the nature of the band structure the occupied and unoccupied bands are plotted separately. Fig.2d shows the indirect $(\Gamma \rightarrow A_0)$ band gap of the investigated compound.

Fig.3b & c show partial density of states of 5-zido-1H-tetrazole. In the energy range between –11.4 eV and –11.2 eV the bands are originated from H-1s, N-2s/2p and C-2s/2p states. In this range the strongly hybridized N-2p state and C-2p state are dominant while the contribution H-1s and C-2s states are small. The second group from –10.4 eV to –9.4 eV is mainly due to the N 2s/2p, C 2s/2p and H-1s states. N-2p and C-2s states show dominancy in this range while the contribution of N-2s and C-2s states is negligible. The third group from –8.3 eV to –7.8 eV is the mixture of N 2s/2p, C 2s/2p, H-1s states with leading role of N-2p state. The fourth group in the energy range between –4.6 eV and –3.5 eV the bands are formed by the combination of N-2p states and C-2p states with miner contribution of N-2s and H-1s states. The fifth group from –3.3 eV to –2.6 eV the bands are originated from C-2s/2p states and N-2s/2p states. The sixth group of bands in the energy range between –2.6 eV and –1.4 eV are formed by the contribution of N-2s/2p states, C-2s/2p states. N-2p state is foremost in this range. We should emphasize that N-2s states and C-2s state are strongly hybridized in this range. The group of bands from –0.3 eV up to Fermi level is mostly contributing the valance region formed by N-2p states and C-2p states. The first group of bands above Fermi level is formed by the combination of N-2p and C-2s/2p states. The next group of bands in the energy range between 7.2 eV and 8.0 eV designed by the contribution of N-2p and C-2p states with the foremost role of C-2p states. N-2s/2p and C-2s/2p states contribute in the formation of bands in the energy range from 8.4 eV to 9.4 eV. In this range there is strong hybridization between C-2s and N-2p state as shown in Fig.3(c). In the energy range from 10.0 eV to 11.2 eV the bands are fashioned by the contribution of N-2s/2p, C-2s/2p states and H-1s state with hybridization of N-2p and C-2p states. In the energy range from 11.7 eV to 16.7 eV the contribution of the N-2s/2p states, C-2s/2p states and H-1s state forms bands with hybridization of N-2s and H-1s states. In the energy range between 16.8 eV to 18.4 eV the bands fashioned by the N 2s/2p states, C 2s/2p states and H-1s state. In this range there is strong hybridization between N-s, H-s states and N-2p, C-2p states.

3.2. Electronic charge density

Electronic charge density plot is used for accurate description of bonds nature [59, 60]. The charge density of 5-azido-1H-tetrazole is derived from the reliable converge wave function which is used to study the bonds nature of the solid. The total valance charge density was calculated in $(\bar{4}\ 0\ \bar{9})$ plane using mBJ scheme for complete visualization of charge transfer and bonding properties. Fig.4a shows the three repeated cells of 5-azido-H-tetrazole along Y axis which give the clear image that 5-

azido-H-tetrazole contains four homodimers. In each homodimer the molecules held together by hydrogen bond. The calculated length of the bond between H and N_4 is 1.74 Å as shown in Fig.4b.

(a)

(b)

(c)
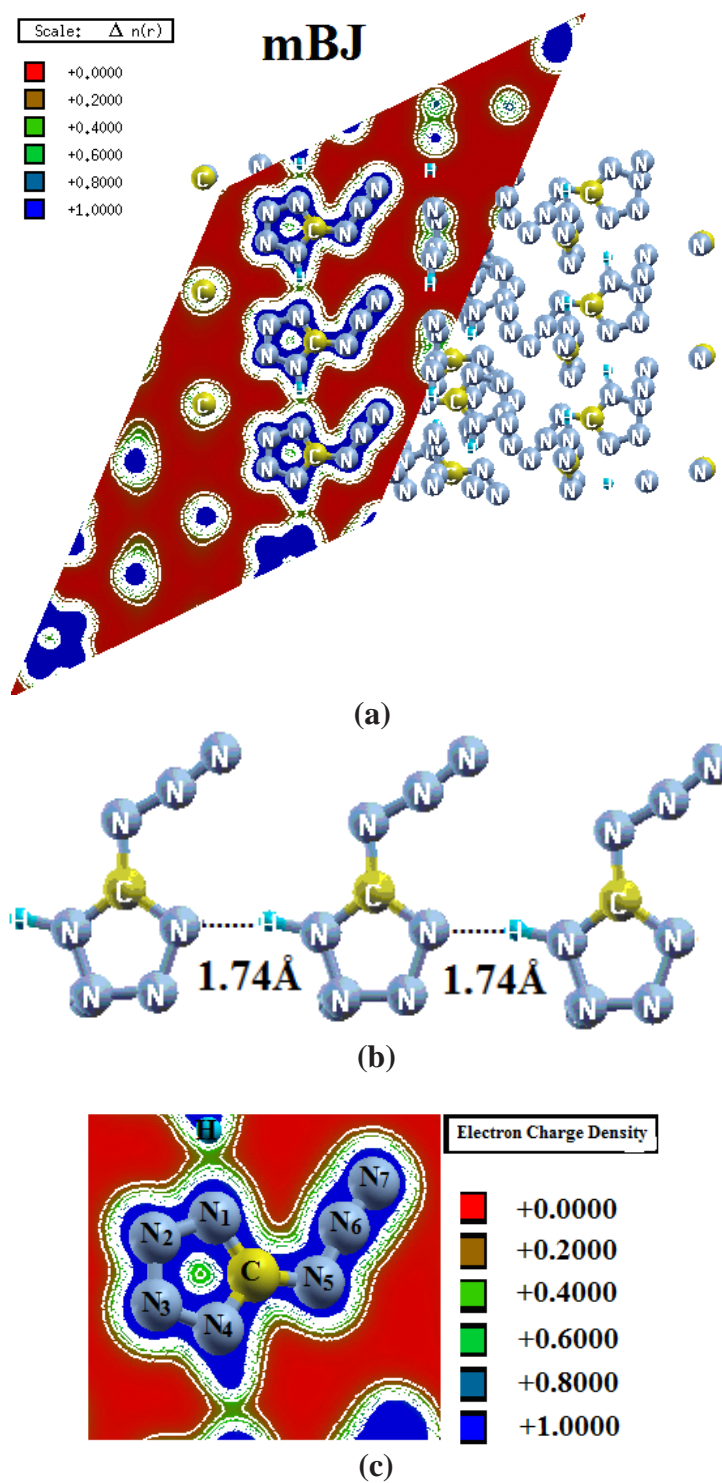
Figure 4. Electronic charge density contour of three repeated cell in $\left(\overline{4}0\overline{9}\right)$ plane using mBJ (b) Homodimer among 5-azido-1H-tetrazole molecules (c) Electronic charge density contour   of single molecule in $\left(\overline{4}0\overline{9}\right)$ plane

The eight formulas in the investigated compound have same number, kind, and order of atoms, therefore, to calculate the electronic charge density only the single molecule is shown in Fig.4c. The strong charge shearing between the atoms of 5-azido-1H-tetrazole molecule show covalent bond. According to Pauling scale the electro-negativity values of C(2.5), N(3.0) and H(2.1) shows that there is covalent bond between the $C–N_1$, $N_1–N_2$, $N_2–N_3$, $N_3–N_4$, $N_4–C$, $C–N_5$, $N_5–N_6$, $N_6–N_7$ and $H–N_1$. The electro-negativity difference in $C–N_1(0.5)$ shows that there is polarity in covalent bond. The cloud around the molecule shows that the intensity of the charge which is mainly due to the delocalized electron [61] resonates on the 5-azido-1H-tetrazole molecule. The calculated bond length, angles and torsion angles of 5-azido-1H-terazole are shown in Table1 and Table 2 which show close agreement to previous reported work of Stierstorfer et al. [19].

Table 1. Calculated bond length and bond angles of 5-azido-1H-tetrazole

Bond length (Å)			Bond angles (°)		
	Present work[*]	Exp. work[a]		Present work[*]	Exp. work[a]
$C_1–N_1$	1.347	1.327	$C_1–N_1–N_2$	108.1	108.3
$N_1–N_2$	1.359	1.355	$N_3–N_2–N_1$	106.9	106.5
$N_2–N_3$	1.307	1.295	$N_2–N_3–N_4$	110.6	110.6
$N_3–N_4$	1.369	1.372	$N_1–C_1–N_5$	121.9	121.0
$N_4–C_1$	1.340	1.321	$C_1–N_4–N_3$	105.5	105.1
$C_1–N_5$	1.380	1.383	$N_4–C_1–N_5$	129.2	129.5
$N_5–N_6$	1.253	1.267	$N_6–N_5–C_1$	114.8	113.1
$N_6–N_7$	1.136	1.117	$N_5–N_6–N_7$	171.2	171.9

[Present work][*], [Stierstorfer et al][a]

Table 2. Calculated torsion angles of 5-azido-1H-tetrazole

Torsion angles (°)	Present work[*]	Exp. work[a]
$N_2–N_1–C_1–N_5$	178.04	178.14
$N_1–C_1–N_5–N_6$	174.69	174.30

[Present work][*], [Stierstorfer et al][a]

3.3. Optical properties

In the history of materials research optical properties of solids and their measurements represent one of the most important scientific performances. There is no possibility to get advancement in photonic devices for optical communication without proper understanding optical properties of the materials. Optical properties of materials attains much attention not only in physics in usual traditional research but also used in other sciences and engineering in wide range [62].

In this work the main aspect for calculation of optical properties is dielectric function. For calculation of frequency dependent dielectric function $\varepsilon(\omega)$ we need energy eigenvalues and electron

wave functions. Both energy eigenvalues and electron wave function are the natural output for the calculation of band structure. The symmetry of the reported crystal structure consent to three non-zero components of second order dielectric tensor along **a**, **b** and **c** crystallographic axis. The three principal complex tensor components for single crystals are $\varepsilon^{xx}(\omega)$, $\varepsilon^{yy}(\omega)$ and $\varepsilon^{zz}(\omega)$. We need to calculate the three components of the imaginary part of dielectric function for complete characterization of linear optical properties using the expression taken from the Ref [63].

$$\varepsilon_2^{ij} = \frac{4\pi^2 e^2}{Vm^2\omega^2} \times \sum_{nn'\sigma} \langle kn\sigma | p_i | kn'\sigma \rangle \langle kn'\sigma | p_j | kn\sigma \rangle \times f_{kn}(1 - f_{kn'}) \delta(E_{kn'} - E_{kn} - \hbar\omega)$$

In the given expression m and e represent mass and charge of electron and ω represent the electromagnetic radiation striking the crystal, V represent volume of the unit cell, in bracket notation p represent the momentum operator, $|kn\sigma\rangle$ represent the crystal wave function with crystal momentum k and σ spin which correspond to the eigenvalue E_{kn}. The Fermi distribution function is represented by f_{kn} makes sure the counting of transition from occupied to unoccupied state and $\delta(E_{kn'} - E_{kn} - \hbar\omega)$ represents the condition for conservation of total energy. Here we ignore phonons involved in the indirect inter-band transition because of small contribution to $\varepsilon_2(\omega)$ and only take direct band transition between occupied and unoccupied state.

(e)

(f)

(g)
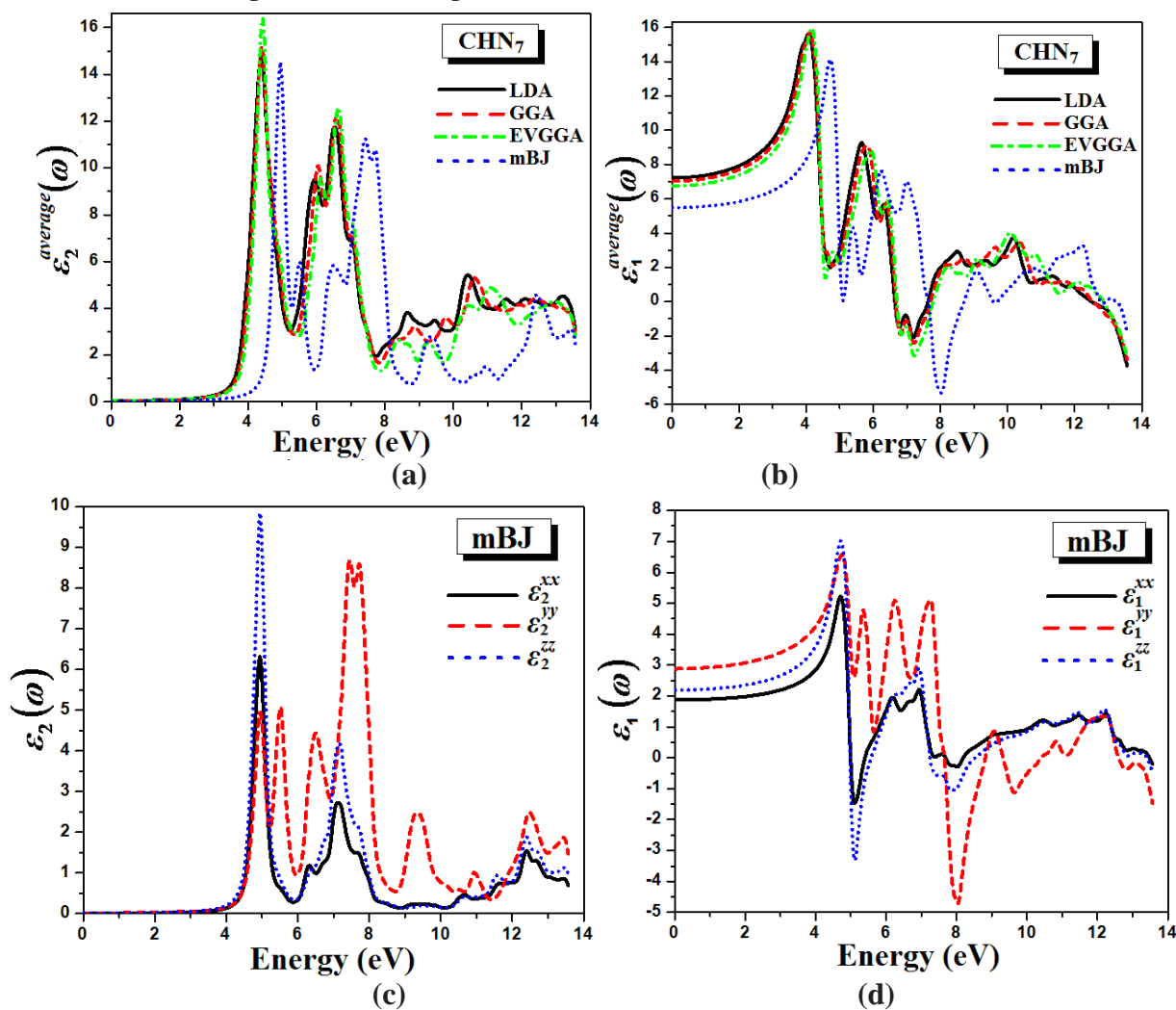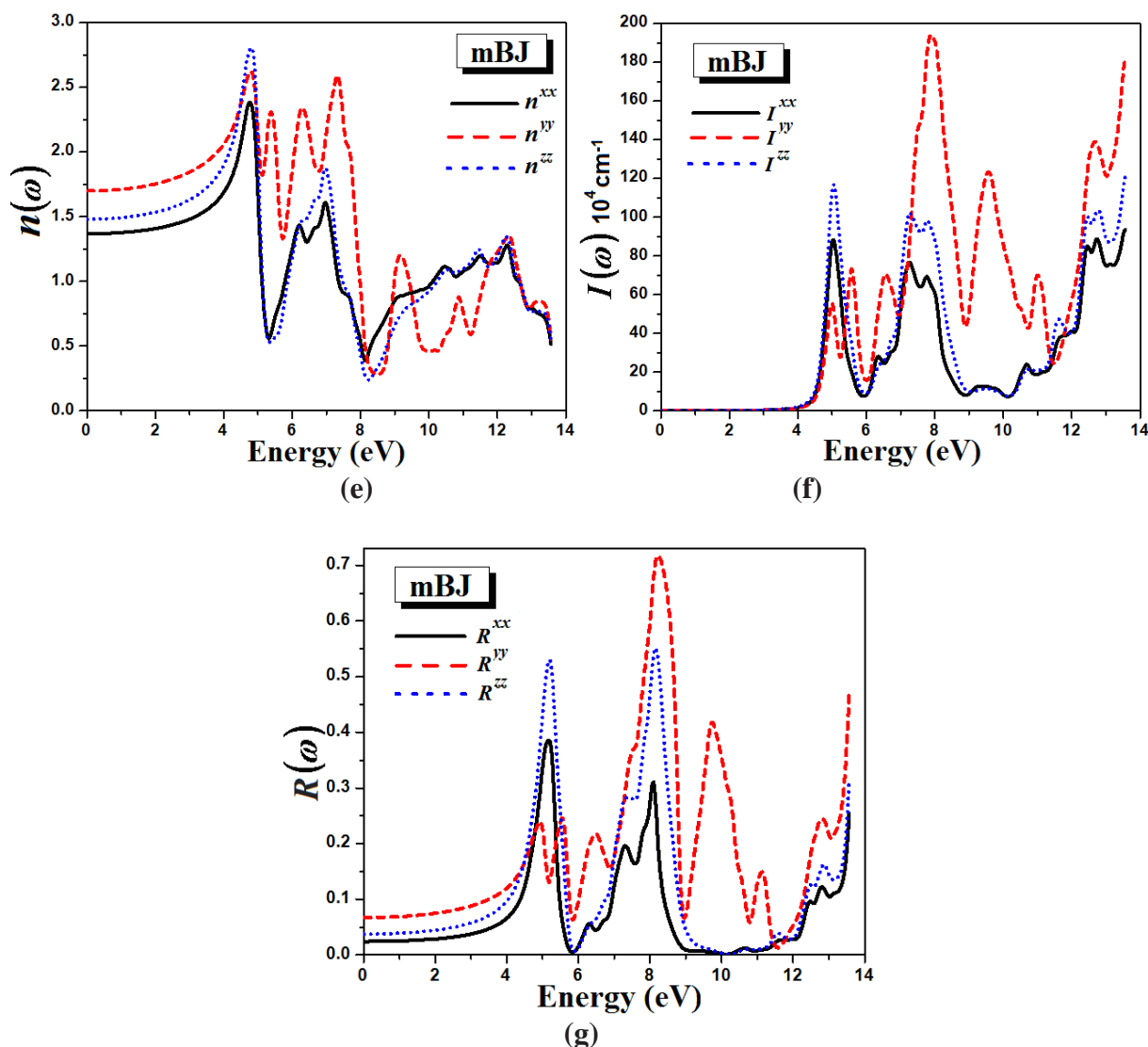
Figure 5. (a) Calculated $\varepsilon_2^{average}(\omega)$ (b) Calculated $\varepsilon_1^{average}(\omega)$ (c) Calculated $\varepsilon_2^{xx}(\omega)$, $\varepsilon_2^{yy}(\omega)$ and $\varepsilon_2^{zz}(\omega)$ (d) Calculated $\varepsilon_1^{xx}(\omega)$, $\varepsilon_1^{yy}(\omega)$ and $\varepsilon_1^{zz}(\omega)$ (e) Calculated $n^{xx}(0)$, $n^{yy}(0)$ and $n^{zz}(0)$ (f) Calculated $I^{xx}(\omega)$, $I^{yy}(\omega)$ and $I^{zz}(\omega)$ (g) Calculated $R^{xx}(\omega)$, $R^{yy}(\omega)$ and $R^{zz}(\omega)$

The average value of these three tensor components is taken for calculation of imaginary part dielectric function. The imaginary part of dielectric function $\varepsilon_2^{average}(\omega)$ can be divided into direct and indirect band transitions. The electric dipole transitions between occupied and unoccupied bands are generally used to determine the peaks in the optical response.

These peaks can be identified using the band structure. The optical spectra of $\varepsilon_2^{average}(\omega)$ is shifted towards higher energies, as one move from LDA to GGA-PBE, EVGGA and mBJ as shown in the Fig.5a. According to Reshak et al.[64] mBJ causes to shift all structures towards higher energy with lower amplitude yields better band splitting. Photons having energy less than 4.43 eV show high transparency and no absorption occurs in this range. At absorption edge first transition of electron occurs from valance band maximum (VBM) fashioned by N-2p and C-2p states to conduction band

minimum (CBM) shaped by N-2p and C-2s/2p states. In the energy range between 4.43 eV and 5.0 eV shows strong photon absorption. In the energy range from 5.31 eV to 6.84 eV the small peaks of the energy spectra show less absorption. The absorption again becomes maximum in the energy range from 6.84 eV to 7.50 eV. In energy range between 8.8 eV and 13.5 eV the small peaks show maximum reflectivity and negligible absorption.

From Kramers-Kronig inversion, the real part of dielectric function can be calculated using imaginary part of dielectric function [65].

$$\varepsilon_1(\omega) = 1 + \frac{2}{\pi} P \int_0^\infty \frac{\omega' \varepsilon_2(\omega')}{\omega'^2 - \omega^2} d\omega'$$

where P represent principal value of integral. The real part of dielectric function $\varepsilon_1^{average}(\omega)$ calculated using LDA, GGA, EVGGA, and mBJ is shown in Fig.5b. One can see that mBJ shifts whole structure towards higher energies in comparison to the almost identical structures of $\varepsilon_1^{average}(\omega)$ obtained by LDA, GGA and EVGGA.

The values of $\varepsilon_1^{average}(0)$ are presented in Table 3. mBJ gives the lowest values. We note that a smaller energy gap yields a larger $\varepsilon_1(0)$ value. This could be explained on the basis of the Penn model [66]. Penn proposed a relation between $\varepsilon_1(0)$ and E_g, $\varepsilon_1(0) \approx 1 + (\hbar \omega_P / E_g)^2$. E_g is some kind of averaged energy gap which could be related to the real energy gap. It is clear that $\varepsilon_1(0)$ is inversely proportional with E_g. Hence a larger E_g yields a smaller $\varepsilon_1(0)$.

Since the investigated compound is monoclinic therefore there exist several principal complex tensor components, we will take only the major components. These are $\varepsilon_2^{xx}(\omega)$, $\varepsilon_2^{yy}(\omega)$ and $\varepsilon_2^{zz}(\omega)$ the imaginary parts of the dielectric function as illustrated in Fig. 5c. There is a considerable anisotropy between the three components of dielectric tensors. At 5.0 eV the three components form the first peak of the optical spectrum, it is clear that $\varepsilon_2^{zz}(\omega)$ component show the highest amplitude as a dominant component and play major role in transition of electron from bottom VB to the top of CB. While $\varepsilon_2^{xx}(\omega)$ and $\varepsilon_2^{yy}(\omega)$ show its maximum value at 6.3 and 5.0.

Table 3. Calculated $\varepsilon_1^{average}(0)$, $\varepsilon_1^{xx}(0)$, $\varepsilon_1^{yy}(0)$, $\varepsilon_1^{zz}(0)$ and E_g for 5-azido-1H-tetrazole

	LDA	GGA	EVGGA	mBJ
$\varepsilon_1^{average}(0)$	7.22	7.08	6.80	5.47
$\varepsilon_1^{xx}(0)$	2.48	2.38	2.28	1.87
$\varepsilon_1^{yy}(0)$	3.77	3.70	3.61	2.89
$\varepsilon_1^{zz}(0)$	2.90	2.86	2.74	2.22
$E_g (eV)$	3.60	3.65	3.69	4.43

In the energy range from 5.22 eV and above $\varepsilon_2^{yy}(\omega)$ is the dominant. $\varepsilon_2^{yy}(\omega)$ show maximum peaks at 7.45 eV and 8.61 eV elucidate that $\varepsilon_2^{yy}(\omega)$ is more responsible for transition of electron in this range. For the whole energy range both of $\varepsilon_2^{xx}(\omega)$ and $\varepsilon_2^{zz}(\omega)$ are isotropic except at 5.0 and 7.0 eV.

From $\varepsilon_2^{xx}(\omega)$, $\varepsilon_2^{yy}(\omega)$ and $\varepsilon_2^{zz}(\omega)$ we have obtained the real parts of the three principal complex tensor components $\varepsilon_1^{xx}(\omega)$, $\varepsilon_1^{yy}(\omega)$ and $\varepsilon_1^{zz}(\omega)$ as shown in Fig.5d. We should emphasize that there is a considerable anisotropy between the three components. The first peaks located at 4.5 eV show isotropy behavior between $\varepsilon_1^{yy}(\omega)$ and $\varepsilon_1^{zz}(\omega)$ components, whereas both of $\varepsilon_1^{yy}(\omega)$ and $\varepsilon_1^{zz}(\omega)$ exhibit anisotropy with $\varepsilon_1^{xx}(\omega)$ component. In the energy range from 4.5 eV and above both of $\varepsilon_1^{xx}(\omega)$ and $\varepsilon_1^{zz}(\omega)$ components exhibits isotopic behaviors, except around 4.5 eV, between 6.5 and 7.0 eV and 7.0 and 8.5 eV, and anisotropic behavior with $\varepsilon_1^{yy}(\omega)$ component. The values of $\varepsilon_1^{xx}(0)$, $\varepsilon_1^{yy}(0)$ and $\varepsilon_1^{zz}(0)$ are listed in Table 3.

The calculated static components of refractive index $n^{xx}(0)$, $n^{yy}(0)$ and $n^{zz}(0)$ having values 1.36, 1.69, 1.47 satisfy the relation $n(0) = \sqrt{\varepsilon_1(0)}$. The three non zero components of refractive index show maximum value at 4.8 eV. In energy range (0-12) eV there is considerable anisotropy among $n^{xx}(\omega)$, $n^{yy}(\omega)$ and $n^{zz}(\omega)$. The two components $n^{xx}(\omega)$ and $n^{zz}(\omega)$ shows weak isotropy at different ranges while $n^{yy}(\omega)$ shows considerable anisotropy with $n^{xx}(\omega)$ and $n^{zz}(\omega)$. From 12.0 to 13.0 eV the three components show isotropic behavior as illustrated in Fig.5e.

The spectral components of absorption coefficient are shown the Fig.5(f). At the absorption edge there is clear isotopic behavior between $I^{xx}(\omega)$, $I^{yy}(\omega)$ and $I^{zz}(\omega)$ components. At energy range between 9.0 eV and 12.5 eV both $I^{xx}(\omega)$ and $I^{zz}(\omega)$ show isotropy where as $I^{yy}(\omega)$ show considerable anisotropy for the whole range. We note that $I^{yy}(\omega)$ is more responsible to show maximum absorption around 8.0 eV.

The spectral components of reflectivity $R^{xx}(\omega)$, $R^{yy}(\omega)$ and $R^{zz}(\omega)$ are shown Fig.5g. There is considerable anisotropy among the components up to 9.6 eV. At energy range between 9.6 eV and 12.5 eV there is isotropy between $R^{xx}(\omega)$ and $R^{zz}(\omega)$, while $R^{yy}(\omega)$ shows considerable anisotropy between $R^{xx}(\omega)$ and $R^{zz}(\omega)$. The spectral components of reflectivity show maximum reflectivity at 8.0 eV. $R^{yy}(\omega)$ show dominancy in this range.

4. CONCLUSION

In this work a DFT study is performed for calculating the electronic and optical properties of 5-azido-1H-tetrazole. The four approximations LDA, GGA-PBE, EVGGA and mBJ were used for exchange correlation potential to calculate the band structure, total and partial density of states which gives clear detail about the orbitals involved in bands formation. The mBJ scheme was selected for better band splitting. The calculated band structure shows that the compound is semiconductor having indirect $(\Gamma \rightarrow A_0)$ band gap of 3.60 eV (LDA), 3.65 eV (GGA), 3.69 eV (EVGGA), and 4.43 eV (mBJ). The band gap's values shows that the investigated compound is suitable for optoelectronic devices in far ultraviolet (UV-C) region. The calculated total valance charge density in $(\overline{4}\ 0\ \overline{9})$ plane shows the covalent nature of the bond in 5-azido-1H-tetrazole molecule. The plot of total valence charge density also gives an idea about the homodimers of 5-azido-1H-tetrazole molecules. The

calculated bond length, bond angles and torsion angles of 5-azido-1H-tetrazole show close agreement with experimental results. The average value of real and imaginary part of dielectric function was calculated. The peaks in calculated spectra of $\varepsilon_2^{average}(\omega)$ shows transition of electron from occupied bands to unoccupied bands. The three principal spectral components of the three principal tensor components of $\varepsilon_2(\omega)$, $\varepsilon_1(\omega)$, $n(\omega)$, $I(\omega)$ and $R(\omega)$ were investigated.

References

1. S.H. Li, H. G. Shi, C. H. Sun, X. T. Li, S. P. Pang, Y. Z. Yu, X. Zhao, J. Chem Crystallogr. 39 (2009) 13
2. F. R. Benson, The high nitrogen compounds. Wiley-Interscience, New York, NY 1984
3. D. E. Chavez, M. A. Hiskey, R. D. Gilardi, *Angew Chem Int Ed*. 39 (2000) 1791
4. J. Kerth, S. Lobbecke, *Propellants Explos Pyrotech*. 27 (2000)111
5. J. Neutz, O. Grosshardt, S. Schaufele, H. Schuppler, W. Schweikert, *Propellants Explos Pyrotech*, 28 (2003)181
6. M. H. V. Huynh, M.A. Hiskey, D.E. Chavez, D.L. Naud, R.D. Gilardi, *J. Am Chem Soc*. 127 (2005) 12537
7. R. P. Singh, R.D. Verma, D.T. Meshri, J.M. Shreeve, *Angew Chem Int Ed*. 45 (2006) 3584
8. M. Smiglak, A. Metlen, R.D. Rogers, *Acc Chem Res*. 40 (2007) 1182
9. J.S. Li, Propellants Explos Pyrotech. 33 (2008) 443
10. T. Wei, W.H. Zhu, X.W. Zhang, Y. F. Li, H.M. Xiao, *J. Phys Chem A*. 113 (2009) 9404
11. Gamal K. Gomma, Materials Chemistry and Physics. 56 (1998) 27
12. K.F. Khaleda, M.M. Al-Qahtanib, Materials Chemistry and Physics. 113 (2009) 150
13. Janez Pirnat, Janko Luznik, Vojko Jazbinšek, Veselko Zˇ agar, Janez Seliger, Thomas M.Klapotke , Zvonko Trontelj, Chemical Physics 364 (2009) 98
14. Chen ZhaoXu, Xiao Heming, Yang Shulin, Chemical Physics. 250 (1999) 243
15. T. M. Klapötke, in: *Moderne Anorganische Chemie*, E. Riedel (Hrsg.), 3. Aufl., Walter de Gruyter, Berlin New York, (2007) 99
16. R. P. Singh, R. D. Verma, D. T. Meshri, J. M. Shreeve, *Angew. Chem. 118* (2006) 3664
17. T. M. Klapötke, in: *High Energy Density Materials*, T. M. Klapötke (Hrsg.), Springer, Berlin Heidelberg, (2007) 85
18. R. D. Chapman, J. W. Fronabarger, R. D. Gilardi, *Tetrahedron* Lett. 47 (2006) 7707
19. J. Stierstorfer, T. M. Klapötke, A. Hammerla, R. D. Chapman, *Z. Anorg. Allg. Chem.* 634 (2008) 1051
20. H.-J. Arpe, (ed), *Ullmannπs Encyclopedia of Industrial Chemistry*, 5th Ed., Vol. A13, Wiley-VCH, Weinheim _ Berlin, (1999), 177
21. C. F Ye, H.X. Gao, J. A. Boatz, *Angew Chem Int Ed*. 45 (2006) 7262
22. M. H. V. Huynh, M.A. Hiskey, J.G. Archuleta, *Angew Chem Int Ed*. 44 (2005) 737
23. D. R. Miller, D.C. Swenson, E. G. Gillan, *J. Am Chem Soc*. 126 (2004) 5372
24. A.N Ali, S. F. Son, M. A. Hiskey, D. L. Naud, *J. Propul Power*. 20 (2004) 120
25. H. S. Jadhav, D. D. Dhavale, V. N. Krishnamurthy, *Theory Pract Engerg Mater*. 4 (2001) 493

26. D. E. Chavez, M. A. Hiskey, D. L. Naud, *J. Pyrotech*. 10 (1999) 17
27. Z. X. Chen, J. M. Xiao H. M. Xiao, Y. N. Chiu, *J. Phys Chem A*. 103 (1999) 8062
28. T. M. Klapo¨tke, *Struct Bond*. 125 (2007) 85
29. T. M. Klapo¨tke, C. M. Sabate´, *Chem Mater*. 20 (2008) 3629
30. T. M. Klapo¨tke, J. Stierstorfer, *J. Am Chem Soc*.131 (2009) 1122
31. Z. X. Chen, H. M. Xiao, *Int J. Quantum Chem*. 79 (2000) 350
32. A. Hammer, T.M. Klapo¨tke, H. No¨th, M. Warchhold, G. Holl, *Propellants Explos Pyrotech*. 28 (2003) 165
33. Y. H. Joo, B. Twamley, S. Garg, J.M. Shreeve, *Angew Chem Int Ed*. 47 (2008) 6236
34. W. Zhu, H. Xiao, *Struct Chem*. 21 (2010) 847
35. W. Friederich, K. Flick, US-Pat. 2179783 (November 14, 1939)
36. Dynamit-Actien-Gesellschaft vormals Alfred Nobel & Co., FRPat. 843916 (July 12, 1939).
37. A. Hammerl, T. M. Klapötke, P. Mayer, J. J. Weigand, *Propellants, Explos., Pyrotech.* 30 (2005) 17
38. A. Hammerl, T. M. Klapötke, *Inorg. Chem.* 41 (2002) 906
39. M. J. Frisch et al, *Gaussian 03, Revision A.1*, Gaussian, Inc., Pittsburgh PA 2003.
40. Suc´eska, M.; *Proc. of 32nd Int. Annual Conference of ICT*, Karlsruhe, (2001), 110
41. http://www.linseis.com
42. http://www.bam.de
43. http://www.reichel-partner.de/
44. S. J. Clark, M. D. Segall, C. J. Pickard, P. J. Hasnip, M. I. J. Probert, K. R. Refson and M. C. Payne, *Z. Kristallogr*. 220 (2005) 567
45. D. Vanderbilt, *Phys Rev B*. 41 (1990) 7892
46. S. Gao, *Computer Physics Communications*. 153 (2003) 190
47. K. Schwarz, *Journal of Solid State Chemistry*. 176 (2003) 319
48. http://www.ccdc.cam.ac.uk/cgi-bin/catreq.cgi
49. P. Balaha, K. Shewartz, G. K. H. Madsen, D. Kvsnicka, J. Luitz, WIEN2K, an augmented wave +local orbitals program for calculating crystals properties, Karlheinz Schewartz, Techn. Universitat, Wien Austria, 2001, ISBN 3-9501031-1-2.
50. D. M. Ceperley, B. I. Alder, *Phys. Rev. Lett*. 45 (1980) 566
51. J. P. Perdew, K. Burke, M. Ernzerhof, *Phys. Rev. Lett*. 77 (1996) 3865
52. E. Engel, S. H. Vosko, *Physical. Rev. B*. 47 (1993) 13164
53. Tran F. and Blaha P, Phys. Rev. Lett. 102 (2009) 226401
54. I. Khan, I.Ahmad, D. Zhang, H. A. Rahnamaye Aliabad, S. J. Asadabadi, Journal of Physics and Chemistry of Solids. 74 (2013) 181
55. A. H. Reshak, H. Kamarudin, S. Auluck, I.V. Kityk *Journal of Solid State Chemistry*.186 (2012) 47
56. S. Hardev, S. M. Singh, A. H. Reshak, M. K. Kashyap, *Journal of Alloys and Compounds*. 518 (2012) 74
57. T. Ouahrani, R. Khenata, B. Lasri, A. H. Reshak, A. Bouhemadou, S. Bin-Omran, *Physica B*. 407 (2012) 3760
58. A. H. Reshak, I. V. Kityk, R. Khenata, S. Auluck, *Journal of Alloys and Compounds*. 509 (2011) 6737
59. R. Hoffman, *Rev. Mod. Phys*. 60 (1988) 601
60. C. D. Gellatt, A. R. Jr. Willaims, V. L. Moruzzi, Phys. Rev. B. 27 (1983) 2005
61. A. Hammerl, T. M. Klapötke, H. Nöth, M. Warchhold, Propellants, Explosives, Pyrotechnics. 28, No.4 (2003) 165
62. J. Singh, "Optical Properties of Condensed Matter and Applications" John Wiley & sons,England, *2006.* ISBN-13 978-0-470-02192–7 (HB)
63. A. Delin, P.Ravindran, O. Eriksson, J.M. Wills, Int. J.Quant. Chem. 69 (1998) 349

64. A. H. Reshak, H. Kamarudin, S. Auluk, *J. Phys. Chem. B*. 116 (2012) 4677
65. H. Tributsch, Naturforsch. A. 32A (1977) 972
66. D.R. Penn, *Phys. Rev. B*.128 (1962) 2093